Available online at www.sciencedirect.com
SCIENCE DIRECT®
Thin Solid Films 458 (2004) 9–14
thin solid films
www.elsevier.com/locate/tsf

Fabrication and characterization of polymer/nanoclay hybrid ultrathin multilayer film by spin self-assembly method

Ho-Chul Lee[a,*], Tae-Woo Lee[b,1], Tae-Ho Kim[c], O.Ok Park[c]

[a]*Mobile Part, Coating Laboratory, Samsung Corning Co. Ltd., 644 Jinpyeong-dong, Gumi-si, Gyeongsangbuk-do 730-725, South Korea*
[b]*Center for Advanced Functional Polymers, Korea Advanced Institute of Science and Technology, 373-1, Guseong-dong, Yuseong-gu, Daejeon 305-701, South Korea*
[c]*Department of Chemical and Biomolecular Engineering, Korea Advanced Institute of Science and Technology, 373-1, Guseong-dong, Yuseong-gu, Daejeon 305-701, South Korea*

Received 24 March 2003; received in revised form 16 October 2003; accepted 10 November 2003

Abstract

We have prepared ultrathin multilayer nanostructural films by a layer-by-layer spin self-assembly method using poly (p-phenylene vinylene) (PPV)/layered silicate and characterized them by contact angle measurement, surface dying technique, UV/Vis spectroscopy, photoluminescent (PL) spectroscopy, X-ray reflectivity (XRR), and model-fitting. The hybrid ultrathin multilayer film was stepwisely deposited using the electrostatic forces between the cationic PPV precursor and the negatively charged surface of layered silicate, and finally thermally converted to $(\text{PPV/Laponite RD})_n$ film. The surface coverage of the PPV precursor onto layered silicate and vice versa could be clearly observed using the contact angle measurement and surface dying technique. The continuous increase of UV/Vis absorbance and PL intensity of the films with each bilayer demonstrated the regular and reproducible deposition of this system, and the Kiessig fringes and Bragg peaks in XRR spectra indicated the well-ordered internal structure.
© 2003 Elsevier B.V. All rights reserved.

Keywords: Spin self-assembly; Light-emitting diode; Ultrathin multilayer film; Poly (*p*-phenylene vinylene); Layered silicate

1. Introduction

There is presently increasing interest in polymeric ultrathin multilayer films due to their potential applications to advanced optical and electronic coating [1,2], and rather recently, to optoelectronic devices [3–7]. The polymeric ultrathin multilayer films have been fabricated mainly by the Langmuir–Blodgett (LB) method [8–11] and the self-assembly (SA) method [12–19]. In particular, the SA method can be applied to various charged materials such as charged colloidal particles and polyelectrolytes. Moreover, the SA procedure is very simple and no special apparatus is required. However, the general dipping SA technique requires a long dipping retention time to sufficiently cover the surface with oppositely charged materials because the charged materials adsorb onto the oppositely charged surface only by diffusion. Therefore, although depending on various experimental parameters, it takes at least 10 min to deposit one layer.

Recently, researchers have introduced and adopted the alternative spin SA method [20], consisting of six steps: (1) dropping of charged materials on the substrate; (2) spin-coating; (3) spin-washing; (4) dropping of oppositely charged materials; (5) spin-coating; and (6) spin-washing. In the spin SA method, the adsorption and rearrangement of adsorbed materials onto the surface and the elimination of weakly bound materials are almost simultaneously achieved at a high spinning speed for a short time [20]. By the spin SA method, the multilayer films with highly well-ordered internal structures could be successfully fabricated in oppositely charged polyelectrolytes [20–22] and polyelectrolyte and inorganic spheric nanoparticles [20].

*Corresponding author. Fax: +82-54-470-7814.
E-mail addresses: hochul77.lee@samsung.com (H.-C. Lee), twlee@lucent.com (T.-W. Lee).
[1] *Present address* Bell Laboratories, Lucent Technologies, Rm. 1D-322, 600 Mountain Ave., Murray Hill, NJ 07974, USA.

0040-6090/04/$ - see front matter © 2003 Elsevier B.V. All rights reserved.
doi:10.1016/j.tsf.2003.11.117

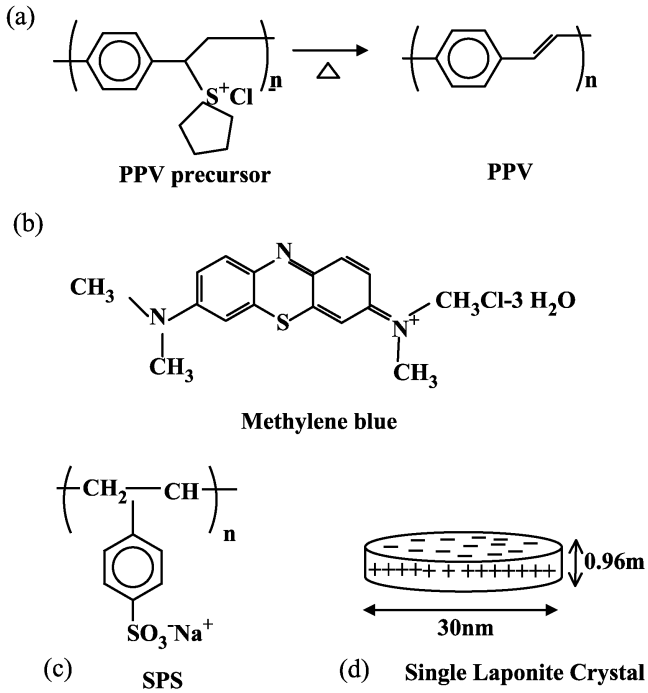

Fig. 1. Chemical structures of (a) PPV precursor and PPV (b) methylene blue (c) SPS (d) single Laponite RD crystal.

In this research, the fabrication and characterization of nanostructural ultrathin multilayer films of poly (*p*-phenylene vinylene) (PPV)/layered silicate via the spin SA method are the focus of interest. The PPV/layered silicate hybrid system can combine the functionality of PPV as a semiconducting fluorescent polymer with that of layered silicate as a gas barrier against oxygen and moisture [23], so that PPV/layered silicate hybrid multilayer ultrathin film is very attractive for optoelectronic devices such as light-emitting diodes. Two-dimensional layered silicate with a large aspect ratio can effectively block the gas penetration [23] such as oxygen and moisture due to the torturous zigzag diffusion and hence can markedly improve the environmental stability of conjugated polymer [23–25]. From this viewpoint, our group has been interested in hybrid materials of conjugated polymer/inorganic layered material.

2. Experimental section

We synthesized the PPV precursor, according to the procedure described elsewhere [23], and one-tenths methanol-diluted PPV precursor was used for the spin SA. SPS was purchased from Aldrich Co. and used as received (10 mM in HPLC water). The concentrations of all the polymer solution are quoted with respect to the monomer repeat unit. The chemical structures used in this study are shown in Fig. 1. The layered silicate used is a mica-type synthetic hectorite, Laponite RD, which has a 0.96 nm thickness and about a 30 nm diameter. A colloidal dispersion of Laponite RD into each exfoliated sheet (0.1 g in 100 ml HPLC water) was achieved by stirring and sonication. The glass substrates for the deposition of cationic PPV precursor were initially sonicated with chloroform, acetone, and methanol (all HPLC grade), and hydrophilized with 1% Chem-solv solution (aqueous alkaline alcohol) to generate negative charges on the surface. The overall process of the layer-by-layer spin SA [20] consists of a cyclic repetition of the following steps at a spinning speed of 2000 rev./min: (1) dropping of positive charged PPV precursor solution on the substrate; (2) spin-coating; (3) spin-washing; (4) dropping of colloidally dispersed Laponite RD with negative surface; (5) spin-coating; and (6) spin-washing. The overall procedure of the spin SA is sketched in Fig. 2. The ultrathin film deposition in the spin SA process is very fast as shown in Fig. 2 and might be explained by considering the fluid rheology, solvent evaporation, and electrostatic attraction between the materials in the dropped solution and the oppositely charged surface. The materials in the highly diluted solution are pulled toward the oppositely charged surface by electrostatic force, and in the spinning process, the solution is spread out thinly with the solvent evaporating. As the solvent evaporates at the high spinning speed, the materials are concentrated and immobilized. Furthermore, additional electrostatic attraction helps the materials to be deposited more rapidly and strongly. The following spin-washing process removes the weakly bound materials, keeping the surface smoother.

In our system, the positive material is cationic PPV precursor and the negative material is layered silicate, Laponite RD, with the negative surface charge. The stepwise deposition of alternate PPV precursor and Laponite RD was carried out using the electrostatic attraction, and final $(\text{PPV/Laponite RD})_n$ hybrid films were obtained by thermally converting the above $(\text{PPV precursor/Laponite RD})_n$ film at 230 °C in vacuo for 3 h.

An Erma model G-I type for static contact angle measurement, a surface dying technique for investigating the degree of surface coverage, a JASCO V-530 UV/Vis spectrophotometer for UV/Vis spectra, a Perkin–Elmer luminescence spectrometer LS 50 for spectra photoluminescent (PL) spectra, and a high resolution X-ray diffractometer (Rigaku RINT 2000, 18 kW) for X-ray reflectivity (XRR) measurement were employed.

3. Results and discussion

The contact angle is directly related to the surface energy, and the surface energy is largely affected by the surface composition. Therefore, in the alternating multilayer film of PPV precursor and Laponite RD, the regular and observable changes in the contact angle

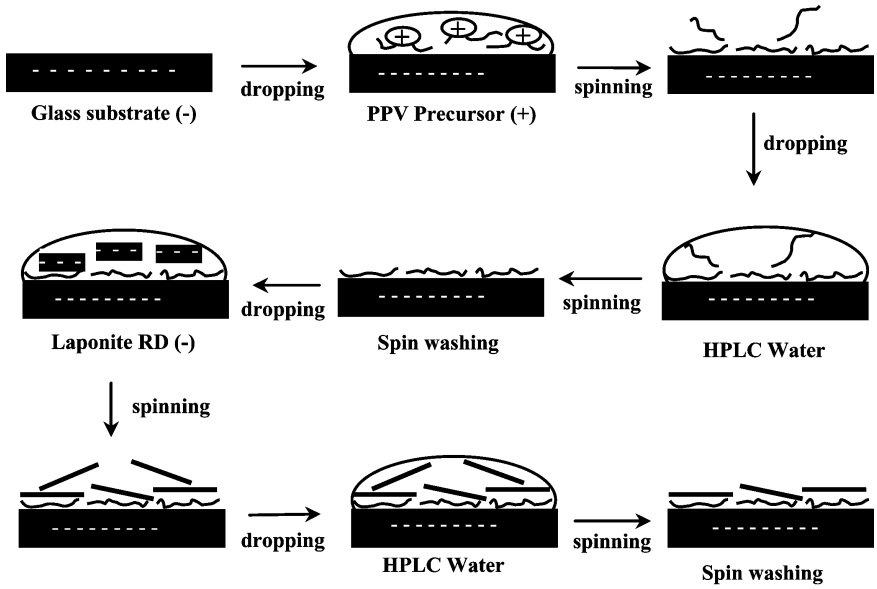

Fig. 2. The overall procedure of spin SA in this experiment.

indicate that the surface is stepwisely deposited with PPV precursor and Laponite RD. Fig. 3 clearly shows the distinct oscillations of the contact angles as the outermost layer is alternating between PPV precursor and Laponite RD, revealing that the surface coverage of PPV precursor by Laponite RD and vice versa is enough to change the surface wettability sharply. Moreover, the fact that the difference of the right and left contact angles of the droplet was negligible and that the contact angles measured at three different locations were nearly the same demonstrates that the surface is uniformly deposited.

Fig. 4 illustrates the UV/Vis absorbance change of the hybrid multilayer films with the number of build-up cycles while the inset exhibits the continuous increase of UV/Vis absorbance at maximum peak. The continuous increase of the optical density of the films with each bilayer demonstrates the stepwise growth of multilayer film with the sequential spin SA.

By surface dying technique, the degree of surface coverage could be investigated. When the outermost layer was negative Laponite RD, positive methylene blue dye ($\lambda_{max}=660$ nm) might adsorb onto the all negative site on the surface except the positive sites where Laponite RD did not cover and PPV precursor

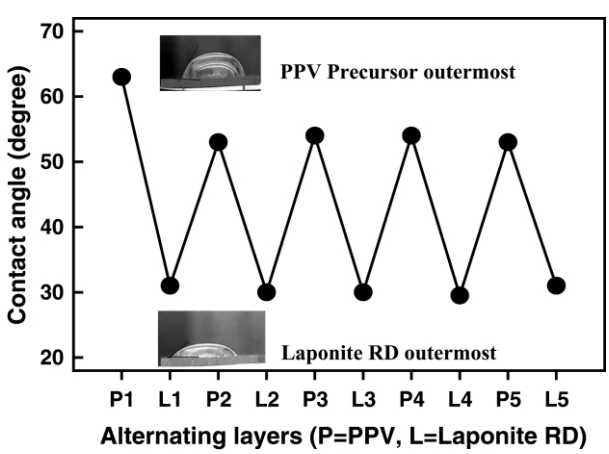

Fig. 3. Water contact angles measured from PPV precursor/Laponite RD hybrid multilayer film via spin SA, where P means PPV precursor outermost layer and L means Laponite RD outermost layer. Inset shows the actural water drops on the PPV precursor and Laponite RD and the contact angles.

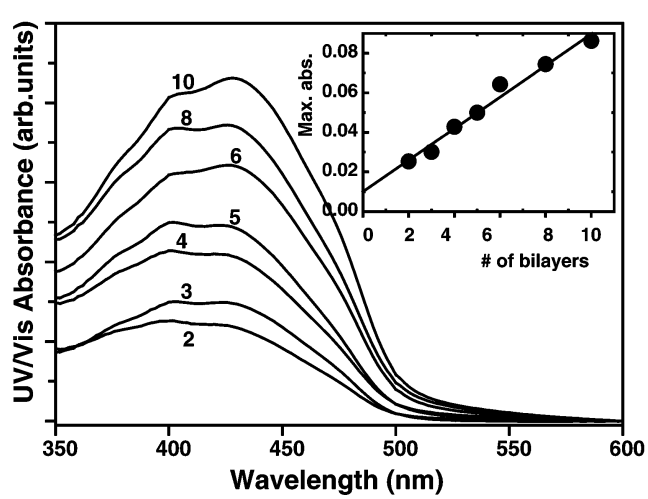

Fig. 4. UV/Vis absorbance change of the hybrid multilayer films with the number of build-up cycles. Inset exhibits the continuous increase of UV/Vis absorbance at the maximum peak.

was exposed to the surface. Additionally, when the outermost layer was covered with positive PPV precursor, positive methylene blue dye might be repelled, only adsorbed onto the sites where PPV precursor did not cover and Laponite RD was exposed to the outer surface. Although, we cannot calculate the degree of surface coverage by each other quantatively, PPV precursor takes up most of the negative sites on Laponite RD as shown in the UV/Vis spectra of Fig. 5. If the plate-like sheets of Laponite RD completely cover the PPV precusor pre-deposited surface, it can be estimated that PPV precursor cover roughly 11 negative site of 12 sites by simply comparing the methylene blue absorbances at 660 nm. For more detailed information on the degree of surface coverage, a more careful and quantative experiment is currently being conducted.

Furthermore, to investigate the degree of interpenetration between the adjacent layers [26,27], three samples with bilayers 2, 4, and 6 were prepared. In addition, we measured their UV/Vis absorption spectra, PL spectra excited at 400 nm, and relative PL quantum efficiency (PLQE) obtained by normalizing the PL spectra of each multilayer film by the absorbance at the PL excitation wavelength of 400 nm. Fig. 6 shows the UV/Vis absorption spectra (norm.) and PL intensity (norm.) of the hybrid multilayer films with bilayers 2, 4, and 6. As the thickness increases linearly with the number of bilayers, two characteristic features appeared: (1) the overall red shift of the spectra was observable in both UV/Vis absorption spectra and PL spectra; and (2) the spectra at long wavelengths increased stepwisely in both UV/Vis absorption spectra and PL spectra. Fig. 7 shows

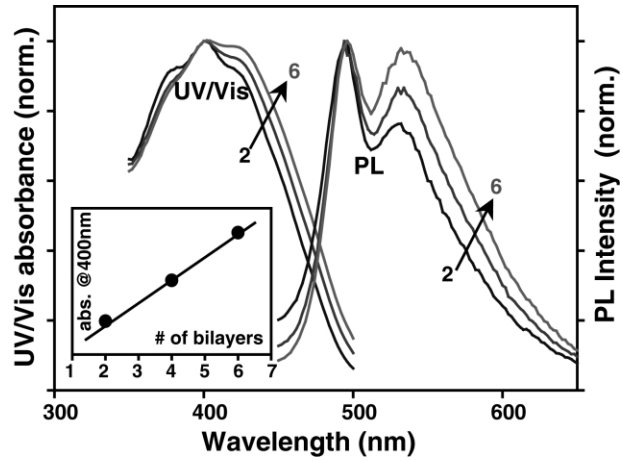

Fig. 6. The normalized UV/Vis absorption spectra and PL spectra with bilayers 2, 4, and 6. Inset shows the linear increase of UV/Vis absorbance at 400 nm of above samples.

the PL spectra and relative PLQE of the above three samples, where the inset shows the gradual increase in PL intensity and the sequential decrease in relative PLQE with the number of bilayers. The above overall features of red shift, increase at long wavelengths of UV/Vis and PL spectra, and gradual decrease of relative PLQE with the number of bilayers could be explained by interlayer interaction due to interpenetration as shown in the inset of Fig. 7, as already reported by Baur et al. [26] and Wang et al. [27]. When the interpenetration between the adjacent layers occurs, PPV can communicate with other PPV, resulting in the additional interlayer

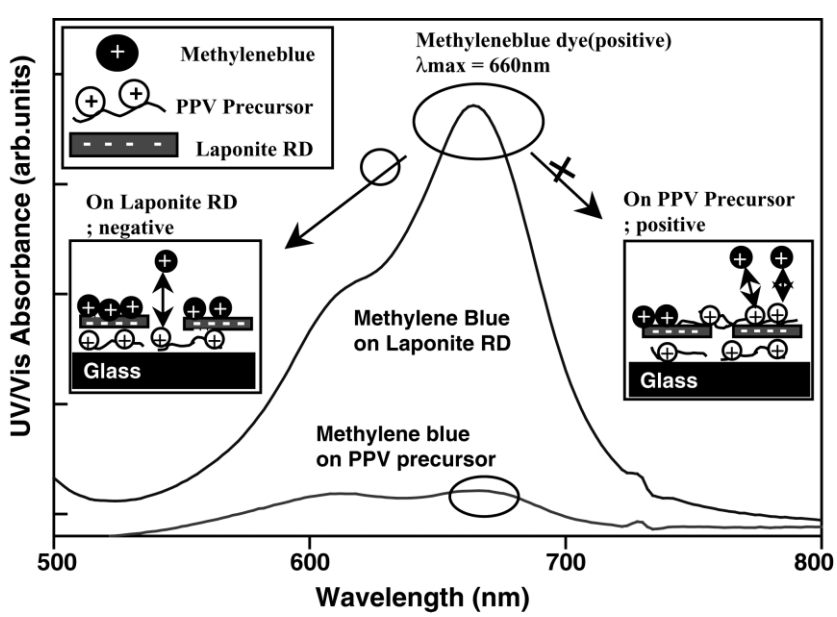

Fig. 5. UV/Vis absorption spectra comparing the amount of methylene blue adsorbed onto the outermost surfaces of PPV precursor and Laponite RD. Inset shows the surface coverage and deposition of methylene blue onto the outer surfaces of PPV precursor and Laponite RD.

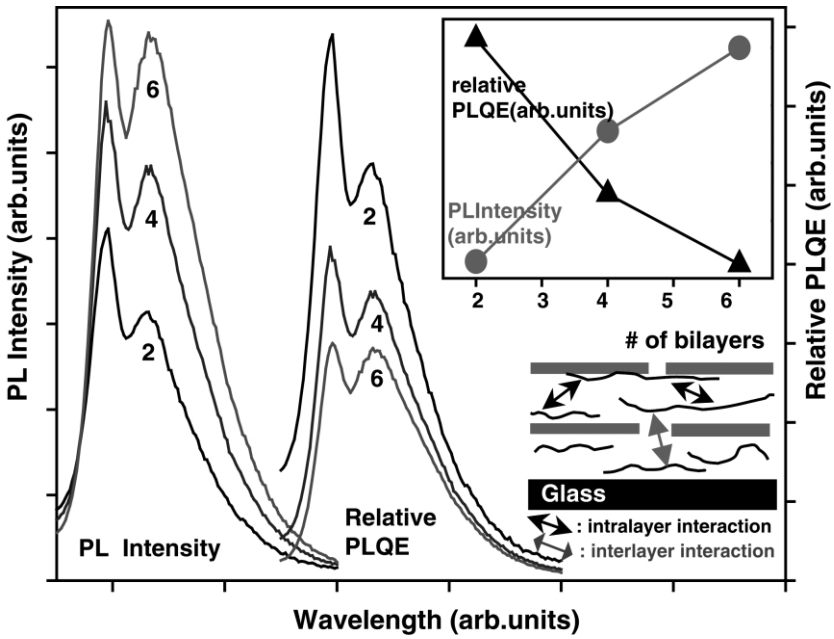

Fig. 7. The PL intensity and relative PLQE spectra with bilayers 2, 4, and 6. Inset shows the gradual increase of PL intensity and sequential decrease of relative PLQE.

interaction. Therefore, the red-shifted, long-wavelength enhanced feature in both UV/Vis and PL spectra could be possible. Moreover, the enhanced interchain interaction due to interpenetration might increase the PL self-quenching due to the more frequent formation of non-emissive interchain excited states, resulting in the gradual decrease in relative PLQE with the number of bilayers.

Fig. 8a exhibits the typical XRR spectra of spin self-assembled films with 2, 5, 8 and 10 bilayers on general microscope slide glass, where the inset shows the linearity between the total film thickness and the number of bilayers with the slope of 3.8 nm. In Fig. 8b, the open circles are the actual data obtained from Rigaku RINT 2000, and the solid lines are from theoretical fit lines. In the sample of $[(PPV/SPS)_4(PPV/Laponite\ RD)_1]_4$, the model fitting was performed in the range from $2\theta = 0.2$ to $1.1°$ because no further Kiessig fringes were detected over $2\theta = 1.1°$. All XRR spectra clearly showed the Kiessig oscillations due to the interference of beams reflected from the upper and the lower interfaces as shown in the inset of Fig. 8b, indicating that the respective layers have distinct interfaces and rather smooth surface roughness. To confirm the internal structure, we prepared $[(PPV/SPS)_6/(PPV/Laponite\ RD)_1]_3$ and $[(PPV/SPS)_4/(PPV/Laponite\ RD)_1]_4$ on silicon wafer. In this case, X-ray recognizes these samples as (polymer I/Laponite RD)$_3$ and (polymer II/

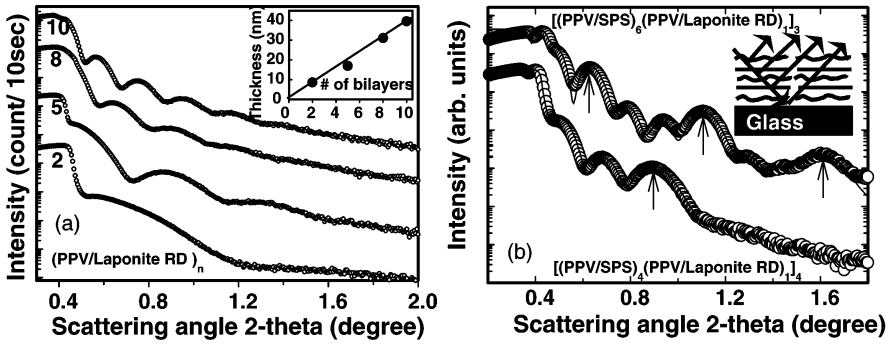

Fig. 8. X-Ray reflectivity of multilayer films of (a) (PPV/Laponite RD)n with 2, 5, 8, 10 bilayers on glass and (b) $[(PPV/SPS)_6/(PPV/Laponite\ RD)_1]_3$ and $[(PPV/SPS)_4/(PPV/Laponite\ RD)_1]_4$ on silicon wafer (open circles = actual data, solid line = theoretical fit). Inset shows the linear increase of thickness with the number of bilayers estimated from Kiessig fringes and the arrows in Fig. 8b indicate the Bragg peaks for the internal structure.

Laponite RD)$_4$ due to the fact that the X-ray technique is sensitive only to electron density variation [28] and that the polymers have little electron density difference. As clearly shown in Fig. 8b, Bragg peaks could be detectable, corresponding to a periodic building-block, (polymer I/Laponite RD) (17.1 nm) and (polymer II/Laponite RD) (10.6 nm). These thicknesses calculated from the Bragg peaks tolerably agreed to those estimated from the model-fitting (16.9 and 10.4 nm each). The thicknesses of each bilayer, (PPV/Laponite RD) and (PPV/SPS), were somewhat variable, roughly 3.8 nm (PPV/Laponite RD) and 2.0 nm (PPV/SPS). These means that the thicknesses of each bilayer is very dependent on the surface states such as the amount of counter charge, coverage, interdiffusion and so on. In our system, the thickness of (PPV/Laponite RD) bilayer was thicker than that of (PPV/SPS) bilayer, implying that the plate-like Laponite RD covers the previous surface more effectively, with blocking the interdiffusion between the multilayers.

4. Conclusion

Ultrathin well-ordered multilayer films with PPV precursor and Laponite RD could be fabricated easily and rapidly via the spin SA method. The multilayer films showed (i) Bragg peaks in XRR spectra; and (ii) structural regularity, meaning that the film thickness would stepwisely increase per bilyer and the hybrid multilayer films were characterized by contact angle measurement, surface dying technique, UV/Vis spectra, XRR spectra, and model fitting.

Acknowledgments

The authors gratefully acknowledge Dr J. Cho for his helpful advice on the sample preparation. This work was partially supported by the Brain Korea 21 Project.

References

[1] Y. Lvov, S. Yamada, T. Kunitake, Thin Solid Films 300 (1997) 107.
[2] F. Saremi, G. Lang, B. Tieke, Adv. Mater. 8 (1996) 923.
[3] J. Cho, K. Char, S.Y. Kim, J.D. Hong, S.K. Lee, D.Y. Kim, Thin Solid Films 379 (2000) 188.
[4] S. Lee, Y. Kang, C. Lee, Synth. Met. 117 (2001) 257.
[5] R. Neumann, D. Davidov, Acta Polym. 49 (1998) 642.
[6] H. Hong, M. Tarabia, H. Chayet, D. Davidov, E.Z. Faraggi, Y. Avny, R. Neumann, S.J. Kirstein, J. Appl. Phys. 79 (1996) 3082.
[7] J.D. Hong, D. Kim, K. Cha, J.I. Jin, Synth. Met. 84 (1997) 815.
[8] Y.H. Kim, D.B. Wurm, M.W. Kim, Y.T. Kim, Thin Solid Films 352 (1999) 138.
[9] Y. Kim, E. Lee, D.Y. Jung, Chem. Mater. 13 (2001) 2684.
[10] L.H. Wang, W. Wang, W.G. Zhang, E.T. Kang, W. Huang, Chem. Mater. 12 (2000) 2212.
[11] K. Clays, N.J. Armstrong, M.C. Ezenyilimba, T.L. Penner, Chem.Mater. 5 (1993) 1032.
[12] G. Decher, Y. Lvov, J. Schmidt, Thin Solid Films 244 (1994) 772.
[13] G. Decher, J. Hong, J. Schmitt, Thin Solid Films 210 (1992) 831.
[14] Y. Lvov, G. Decher, H. Mohwald, Langmuir 9 (1993) 481.
[15] Y. Lvov, H. Haas, G. Decher, H. Mohwald, A. Kalachev, J. Phys. Chem. 97 (1993) 12835.
[16] E.R. Kleinfeld, G.S. Ferguson, Science 265 (1994) 370.
[17] N.A. Kotov, T. Haraszti, L. Turi, G. Zavala, R.E. Geer, I. Dekany, J.H. Fendler, J. Am. Chem. Soc. 119 (1997) 6821.
[18] D.W. Kim, A. Blumstein, J. Kumar, S.K. Tripathy, Chem. Mater. 13 (2001) 243.
[19] D.W. Kim, A. Blumstein, S.K. Tripathy, Chem. Mater. 13 (2001) 1916.
[20] J. Cho, K. Char, J.D. Hong, K.B. Lee, Adv. Mater. 13 (2001) 1076.
[21] S.S. Lee, J.D. Hong, C.H. Kim, K. Kim, J.P. Koo, K.B. Lee, Macromolecules 34 (2001) 5358.
[22] P.A. Chiarelli, M.S. Johal, J.L. Casson, J.B. Roberts, J.M. Robbson, H.L. Wang, Adv. Mater. 13 (2001) 1167.
[23] H.C. Lee, T.W. Lee, Y.T. Lim, O.O. Park, Appl. Clay Sci. 21 (2002) 287.
[24] T.W. Lee, O.O. Park, J.J. Kim, J.M. Hong, Y.C. Kim, Chem. Mater. 13 (2001) 2217.
[25] T.W. Lee, O.O. Park, J. Yoon, J.J. Kim, Adv. Mater. 13 (2001) 211.
[26] J.W. Baur, M.F. Rubner, J.R. Reynolds, S. Kim, Langmuir 15 (1999) 6460.
[27] H.L. Wang, D.W. McBranch, V.I. Klimov, R. Helgeson, F. Wudl, Chem. Phys. Lett. 315 (1999) 173.
[28] M. Tarabia, H. Hong, D. Davidov, S. Kirstein, R. Steitz, R. Neumann, Y. Avny, J. Appl. Phys. 83 (1998) 725.